JOURNAL OF MECHANICS OF CONTINUA AND MATHEMATICAL SCIENCES
www.journalimcms.org

ISSN (Online) : 2454 -7190 Vol.-20, No.-12, December (2025) pp 93-113 ISSN (Print) 0973-8975

FUEL CHARACTERIZATION AND COMPATIBILITY ASSESSMENT OF BERGAMOT PEEL OIL–DIESEL BLENDS FOR CI ENGINE APPLICATIONS

K. Karthikeyan[1], M. Thambidurai[2]

[1,2] Mechanical Engineering, FEAT, Annamalai University, India-608002.

Email: [1]kknvadalur@gmail.com, [2]thambidu@gmail.com

Corresponding Author: **K. Karthikeyan**

https://doi.org/10.26782/jmcms.2025.12.00007

(Received: September 12, 2025; Revised: November 22, 2025; December 04, 2025)

Abstract

The present study explores the feasibility of utilizing Bergamot Peel Oil (BPO) as a renewable alternative to conventional diesel fuel in a compression ignition engine. Before engine testing, the physicochemical properties of BPO were tested. FTIR analysis confirmed the presence of oxygenated functional groups such as esters and carbonyl compounds, while CHNS analysis revealed a significant oxygen content, supporting improved combustion characteristics. GC-MS analysis identified major fatty acid methyl esters contributing to the high volatility and calorific value of BPO. Experimental investigations were conducted at varying blending ratios (BPO10, BPO20, BPO30, BPO40, and BPO50) without any engine modifications, evaluating performance, combustion, and emission parameters against baseline diesel. Results indicated an improvement in brake thermal efficiency (BTE) by 3–6% for BPO30–BPO40 blends, while brake specific fuel consumption (BSFC) reduced by up to 9% for higher blends, attributed to better energy content and oxygenation. In-cylinder analysis revealed increased peak pressure and rate of pressure rise (RoPR) with BPO addition, with BPO50 recording the highest peak due to superior oxidation and localized high temperatures. Ignition delay showed a slight increase for higher blends due to lower cetane number, though overall combustion duration remained comparable to diesel. On the emissions front, smoke opacity was significantly reduced by 14–17% for BPO50 owing to enhanced soot oxidation. Carbon monoxide (CO) and unburned hydrocarbons (HC) decreased by 8–12% across all blends, while NOx emissions exhibited a 6–10% rise for higher blends due to an increase in in-cylinder temperatures and oxygen availability. The findings suggest that BPO, with its oxygenated nature and favorable volatility, can partially replace diesel fuel without major engine modifications, particularly in blends up to BPO40, ensuring improved efficiency and cleaner combustion.

Keywords: Bergamot peel oil, Fuel characterization, Diesel, Engine, Performance.

I. Introduction

The global urgency to reduce greenhouse gas emissions, reduce reliance on fossil fuels, and comply with stringent emission standards such as BS-VI has accelerated the exploration of alternative, renewable fuels for compression ignition (CI) engines. Diesel engines, despite their robustness and efficiency, are scrutinized for their environmental impact, and there is mounting interest in identifying sustainable, low-carbon fuels that can serve as viable substitutes or blend stocks. Among these, bio-based oils, especially those with inherently low viscosity, have gained prominence owing to their favorable fuel properties and compatibility with modern diesel combustion systems.

Over the last five years, there has been a pronounced acceleration in research exploring low-viscosity biofuels, especially essential oils and plant-derived oils, as blendstocks for diesel engines. These studies collectively address both the fuel property enhancements and the operational outcomes when used as partial diesel substitutes, with a growing preference for blends that maintain engine durability while reducing emissions and fossil fuel dependency. Eucalyptus oil blends have attracted widespread interest due to their inherently low viscosity and high volatility. Ellappan and Rajendran demonstrated that a 20% eucalyptus oil–diesel blend decreased kinematic viscosity from 2.9 mm^2/s for pure diesel to 2.3 mm^2/s, resulting in finer fuel atomization and a 4% increase in brake thermal efficiency (BTE), with CO and smoke emissions reduced by 18% and 22%, respectively, compared to conventional diesel. In a complementary study, Patel, Agrawal, and Rawal compared eucalyptus oil blends at 10%, 20%, and 30%, noting that while BTE and NOx emissions improved at lower blend levels, blends above 30% saw a drop in cetane number (from 48 to 43) and a 7% increase in HC emissions, highlighting the critical need for blend optimization. Another recent study by Chivu et al. revealed that eucalyptus oil–diesel blends improved torque at low speeds and reduced BSFC at high loads, though BTE dropped at higher speeds/loads. Notably, 10EU90D achieved up to 60% lower smoke opacity, indicating strong emission benefits alongside partial fossil CO_2 substitution.

Citrus peel oils such as lemon and orange have also shown promise. Ashok et al. provided a comprehensive study, underscoring that introducing lemon oil at 20% by volume reduced the blend's viscosity from 3.6 to 2.6 mm^2/s, improved cold flow properties, and decreased particulate emissions by 13%. Karthickeyan et al. expanded on this by showing that 20% lemon peel oil blends delivered effective reductions in CO (by 16%) and soot (by 19%), attributed to their high limonene content and oxygenated structure, although NOx emissions increased slightly (by 5%) relative to diesel—a phenomenon also observed by Ashok et al. in orange oil–diesel blends, where higher volatility promoted more complete combustion but required careful control of blend ratios for optimal emissions. Pine oil, a terpene-rich essential oil, has been assessed by Vallinayagam et al., who found that 40% pine oil–diesel blends reduced smoke by up to 25% and improved ignition delay by 2°, yet the cetane number decreased from 50 to 44, which, as demonstrated by the same authors Vallinayagam et al., necessitated cetane enhancer additives (e.g., 2-ethylhexyl nitrate) to maintain cold start performance and compliance with engine manufacturer standards. Similarly, Gad et al. evaluated diesel–mandarin essential oil blends (MO10, MO20) at 1500 rpm, showing reduced

cylinder pressure (3%) and HRR (2.5%), with significant cuts in CO (17–30%), UHC (20–40%), smoke (27–44%), and SFC (5–22%), though NOx rises by 25–45Research by Chen et al. on low-viscosity oils found similar trends: cold flow and volatility improve at moderate blends, with BTE gains of 2-5% and substantial (10-20%) reductions in soot and unburned HC compared to neat diesel. However, excessive blends (>40%) often increased fuel consumption due to lower calorific values.

Comprehensive multi-oil comparisons by Doppalapudi, Azad, and Khan evaluated Tucuma biodiesel blends with ethanol, CNTs, and eucalyptus oil, showing that ethanol-based fuels (DE10, TB10E10) achieved notable NOx reductions of 51.37% and 9% at low loads, respectively, compared to diesel. In another study of multi-oil comparison by Nguyen et al., found that the green binary blend B10C90 (10% WCO biodiesel + 90% cedarwood oil) achieved a BTE of 27.8% vs. 28.1% for diesel and comparable combustion efficiency (99.7%), with slightly higher BSEC (15.4 vs. 12.8 MJ/kW-hr). Analytical investigations by Nanthagopal et al. used FTIR and GC-MS to track the stability and degradation of citrus oil–diesel blends, confirming that oils with higher mono-oxygenated components (e.g., linalool and citronellal) provided more robust oxidation resistance and less tendency toward polymerization.

Current research gaps and thrust areas remain prominent. Most prior studies are limited to essential oils widely available in the market (eucalyptus, lemon, orange, pine oils), and there is a notable lack of compositional and fuel evolution analysis for bergamot peel oil. Furthermore, integration of advanced chemical analytics (FTIR, CHNS) with comprehensive fuel property mapping remains sporadic, and systematic evaluation of blends is not yet addressed. Long-term engine durability with high-oxygen, low-viscosity oils and the operational trade-offs between cetane rating, emission mitigation, and fuel system compatibility are underexamined. In response to these gaps, the present study uniquely combines advanced chemical characterization (FTIR, CHNS, GC-MS) with the systematic preparation and analysis of bergamot peel oil–diesel blends at 10%, 20%, 30%, 40%, and 50%. By thoroughly quantifying fuel properties and establishing empirical blend-performance-emission relationships, this work establishes both the fundamental and applied basis for subsequent in-engine optimization and emissions abatement research. The primary objectives are (1) to characterize bergamot peel oil comprehensively; (2) to map the evolution of key fuel properties as a function of blend ratio; and (3) to identify the blend conditions most favorable for future performance and emission enhancements in CI engines.

II. Fuel Preparation

In the present study, initially, oil was extracted from the bergamot fruit peels, which were collected from the nearby juice shops, using a water distillation process at a laboratory scale. Fig.1 shows the bergamot fruit peel, and Fig. 2 shows the steam distillation setup for the extraction of oil from the peel, respectively.

Fig.1. Bergamot fruit peel

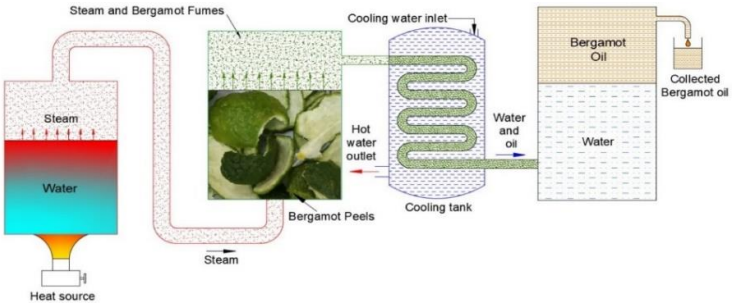

Fig. 2. Steam distillation layout

The oil production unit consists of a steam chamber, where the steam is produced by heating the water through an external heat source. Then, the produced steam is directed to the distillation chamber, half-filled with peels of the bergamot fruit. The steam passes through the peels and carries the oil present in it in the form of fumes into another vessel through a condenser, which contains cold water supplied at a constant rate to condense the fumes and steam. Finally, oil-water condensate is collected in a separate tank where the oil and water form separate layers due to their densities; the water settles at the bottom layer of the tank, and oil floats on the top layer. As the extracted oil is low in viscosity, it can be directly blended with diesel without undergoing any esterification/transesterification process due to the absence of fatty acids. For the experimental investigation, the bergamot peel oil was outsourced from a perfume industry located in Chennai, India.

II.i. Physicochemical properties of BPO and Diesel

The physicochemical properties of BPO were evaluated as per ASTM standards and compared with those of sole diesel, as presented in Table 1. The calorific value of BPO (44.05 MJ/kg) is slightly higher than that of diesel (42.30 MJ/kg), indicating its potential as an energy-rich fuel. The inherent oxygenated nature of BPO is advantageous as it can enhance combustion quality and contribute to reduced CO and HC emissions.

Table 1: Physicochemical properties of sole diesel and BPO

Properties	ASTM	Diesel	BPO	Limit (BS-VI)*
Density (kg/m3)	D1298	835.1	864	820-845
Kinematic viscosity (mm2/s) @ 40°C	D445	2.57	1.62	2-4.5
Flash point (°C)	D93	56	51	Min. 35
Fire point (°C)	D93	62	58	-

Calorific value (MJ/kg)	D420	42.30	44.05	-
Final Boiling point (°C)	D86	150-380	162	-
Cetane Index	D976	49	25	Min. 46

*****Taken from the literature of Duraisamy, Rangasamy, and K. Hossain*

However, the relatively higher density of BPO (864 kg/m³) compared to diesel (835.1 kg/m³) may influence fuel–air mixing, while its lower kinematic viscosity (1.62 mm²/s) can affect spray atomization and lubrication characteristics. Furthermore, BPO shows marginally lower flash and fire points than diesel, which could lead to handling and storage considerations. The cetane index of BPO (25) is significantly lower than that of diesel (49), which may adversely affect ignition quality in compression ignition engines.

II.ii. Blend Preparation

Bergamot peel oil (BPO) was blended with diesel in different volume proportions to evaluate its feasibility as a supplementary fuel. The blending was carried out at ratios of 10:90, 20:80, 30:70, 40:60, and 50:50 (BPO: diesel), and the resulting mixtures were designated as BPO10, BPO20, BPO30, BPO40, and BPO50, respectively. The blends were prepared through volumetric mixing under ambient laboratory conditions to ensure homogeneity without the need for external surfactants or stabilizers, owing to the inherent miscibility of BPO with diesel. The physicochemical properties of these blends, determined in accordance with ASTM standard procedures, are presented in Table 2. These properties serve as a critical baseline for understanding the impact of BPO addition on performance, combustion, and emission characteristics of the test engine.

Table 2.Physicochemical properties of BPO-Diesel blends

Properties	ASTM	BPO10	BPO20	BPO30	BPO40	BPO50
Density (kg/m3)	D1298	838.0	840.9	843.8	846.7	849.5
Kinematic viscosity (mm2/s) @ 40°C	D445	2.47	2.38	2.28	2.19	2.09
Calorific value (MJ/kg)	D420	42.48	42.65	42.82	43.00	43.17
Cetane Index	D976	47	44	42	39	37

III. Experimental Setup

The test engine setup is integrated with the CRDI (Common Rail Direct Injection) system. The CRDI system consists of a fuel filter, a low-pressure pump, a high-pressure pump, a common rail, a pressure regulatory valve, a pressure sensor, an electronic fuel injector with three nozzle holes (make Delphi TVS), and an Electronic control unit (ECU) (Bosch make). The ECU is an open-loop control, where the parameters such as main injection angle, fuel injection pressure, pilot injection quantity, pilot injection angle, and injection duration can be fed into the ECU from a computer as per the user requirements using “Tuner Pro” software interface, even during engine running conditions. Only the fuel injection pressure is increased from 300 bar to 900 bar in this work. The user's desired fuel injection pressure is transmitted to the ECU, which regulates the rail pressure using a signal from the pressure sensor. A fuel line connection is made between the rail and the electronic fuel injector, which

injects the fuel directly into the cylinder pressure given by the user. The schematic view of the experimental setup for the CRDI diesel engine is shown in Fig.3.

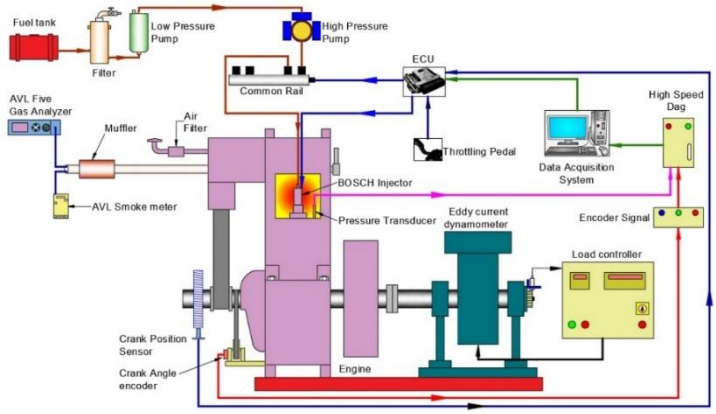

Fig. 3. Test Engine Setup

The CRDI engine is coupled with an eddy current dynamometer for loading purposes. A magnetic pickup sensor sends the signal to the dynamometer speed, which is compared with the engine crank speed by the ECU to ensure the driveshaft consistency, whereas a load cell is employed to measure the test engine torque. This is calibrated by applying a weight equivalent to 24 Nm torque to validate the accuracy and the consistency of the torque analysis. The specification of the CRDI diesel engine is shown in Table 3.

Table 3: Specification of CRDI test engine

Type	**Single cylinder, vertical, water Cooled, 4-stroke VCR DI diesel engine**
Maximum Power Capacity	3.7 kW
Speed of engine	1500 rpm
Bore	80 mm
Stroke	110 mm
Compression ratio	17.5:1
Loading device	Eddy current dynamometer
Fuel Injection type	Modified with electronic fuel injection
Mode of starting	Manually cranking
Injection timing	23°C before TDC

A crank angle encoder was installed on the crankshaft to accurately determine the crank position. Cylinder pressure was recorded using a Kistler piezoelectric pressure transducer, which was mounted during cylinder head assembly. Signals from both the pressure transducer and the crank angle encoder were transmitted to a data acquisition system that synchronized pressure measurements with crank angle positions and stored the data on a computer via Engine Express software. Exhaust emissions, including CO, NO, and HC, were analyzed using a five-gas analyzer. The smoke meter was employed to measure the smoke emission in HSU units. Before testing, the emission analyzer was calibrated with standard reference gases to ensure accuracy.

IV. Results and Discussion

This section presents a detailed analysis of the properties and chemical characteristics of BPO. The performance, emission, and combustion behavior of BPO–diesel blends are evaluated under varying operating conditions. Comparative insights are drawn to highlight the influence of BPO addition on engine characteristics relative to baseline diesel fuel.

IV.i. Characterization of Bergamot Peel Oil

The BPO was subjected to three different analyses, such as CHNS (Carbon, Hydrogen, Nitrogen, and Sulfur) analysis, FTIR (Fourier Transform Infrared Spectroscopy) analysis, and GC (Gas Chromatography) analysis. The CHNS analysis gives the percentage of carbon, hydrogen, nitrogen, and sulfur present in the test substance. The FTIR spectra illustrate absorption bands with characteristic frequency attributed to types of chemical bonds of different functional groups, whilst GC reveals the compounds eluted at different retention times with mass spectra corresponding to compounds present in the test substance.

IV.i.a. CHNS analysis

Fig. 4. represents the CHNS spectra of BPO. Table 5 shows the percentage of carbon, hydrogen, nitrogen, and sulfur content of BPO. It reveals that BPO contains 85.54% carbon, 12.38% hydrogen, 1.47% nitrogen, and no detectable sulfur. The high carbon content indicates that BPO possesses good energy density, making it suitable as a fuel source comparable to conventional hydrocarbons. The appreciable proportion of hydrogen contributes to cleaner combustion by promoting the formation of water vapor and improving the hydrogen-to-carbon ratio, which enhances flame propagation. The nitrogen content is relatively low, suggesting only a minor contribution to NOx formation during combustion. Importantly, the absence of sulfur in BPO highlights its environmental advantage, as it eliminates the risk of SOx emissions, which are major contributors to acid rain.

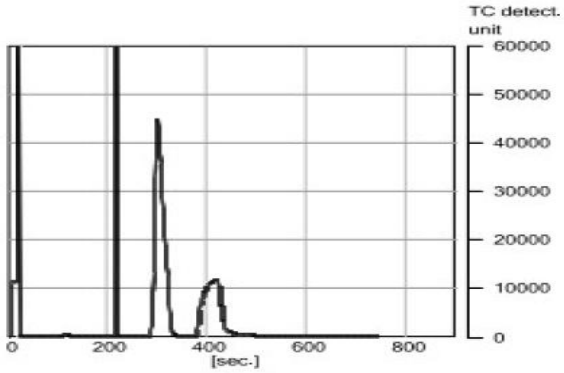

Fig. 4. CHNS analysis of BPO

Table 5: HNS of BPO

Test Fuel	C (%)	H (%)	N (%)	S (%)
Bergamot Peel Oil	85.54	12.38	1.47	0.00

IV.i.b. FT-IR Spectrum of BPO and Diesel

Figure 5 illustrates the FT-IR spectrum of BPO, while Table 6 lists the corresponding functional groups and bond types associated with the observed peaks. The absorption bands at 2920.28 cm^{-1} and 1739.82 cm^{-1} are attributed to C–H stretching vibrations, which indicate the presence of alkane and aromatic groups, respectively. The peak at 1644.34 cm^{-1} is linked to the stretching of C=C bonds, confirming the existence of alkenes. Peaks observed between 1500 cm^{-1} and 500 cm^{-1} fall within the fingerprint region, where bond identification is often ambiguous. Furthermore, the bands at 1442.78 cm^{-1} and 1372.38 cm^{-1} correspond to C–H bending of alkanes and O–H bending of alcohols, respectively. A distinct peak at 1246.04 cm^{-1} is associated with C–O stretching, indicating the presence of oxygenated compounds in BPO. In addition, medium-intensity peaks at 884.38 cm^{-1} and 793.72 cm^{-1} are characteristic of C=C bending vibrations of alkenes. Overall, the FT-IR analysis confirms that BPO consists of paraffins (alkanes), olefins (alkenes), and aromatic compounds.

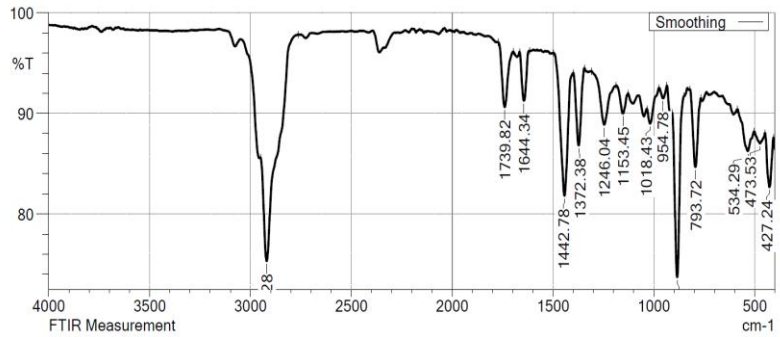

Fig. 5. FT-IR spectra of the BPO

Table 6.FT-IR spectral analysis of BPO

S. No.	Peak cm–1	Intensity (%)	Type of chemical bond	Group
1.	793.72	84.67	C=C bending	Alkene
2.	884.38	73.73	C=C bending	Alkene
3.	1246.04	88.88	C-O stretching	ester
4.	1372.38	86.82	O-H bending	Alcohol
5.	1442.78	81.81	C-H bending	Alkane
6.	1644.34	91.26	C=C stretching	Conjugated Alkene
7.	1739.82	90.63	C-H stretching	Aromatic
8.	2920.28	75.32	C-H stretching	Alkane

IV.i.c. Gas chromatography and Mass Spectroscopy of BPO

The GC–MS spectrum of BPO (Fig. 7) revealed the presence of 58 distinct compounds, predominantly monoterpene hydrocarbons, esters, and alcohols, collectively constituting approximately 92.5% of the oil. Among these, limonene, linalool, and linalyl acetate were identified as the principal components, together contributing nearly 75% of the total composition. These dominant constituents indicate that BPO is rich in unsaturated cyclic and linear hydrocarbons, accompanied by a significant proportion of oxygenated species. The higher oxygen content of these compounds is expected to promote improved fuel reactivity and facilitate more complete combustion compared to conventional hydrocarbons. This compositional profile highlights the potential of BPO as a renewable fuel candidate with intrinsic oxygenation that may help reduce incomplete combustion products such as CO and HC.

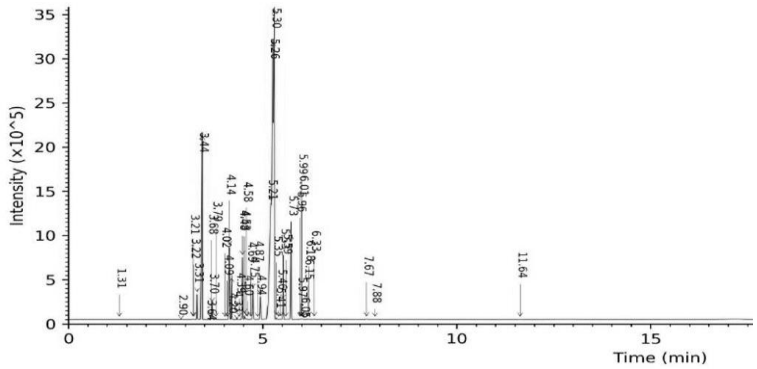

Fig. 7. GCMS spectrum of BPO

IV.ii. Engine characteristics of BPO-Diesel Blends

The engine performance and combustion behavior of bergamot peel oil–diesel blends were systematically evaluated and compared with the sole diesel. Key parameters, including BTE, HC, CO, NO, smoke opacity, in-cylinder pressure, and heat release rate, were analyzed. The results highlight the influence of BPO blends on both performance and emission characteristics of the engine.

IV.ii.a. Brake Thermal Efficiency and Brake Specific Fuel Consumption

The variation of brake thermal efficiency with load for neat diesel and the BPO–diesel blends is shown in Fig. 8. Diesel shows the lowest efficiency across all load points, whereas BPO blends exhibit progressively higher BTE with increasing BPO fraction. Over the test range, BTE for diesel rises from 12.8% at the lowest load to 24.8% at the highest load (3.70 kW). Corresponding BTE values for the 50% BPO blend (BPO50) are 14.5% to 26.4%, respectively, indicating a consistent advantage for BPO - containing fuels. Quantitatively, improvements become apparent even at low loads: at 0.74 kW, the BTE increases from 12.8% (diesel) to 14.5% (BPO50), an absolute increase of 1.7 percentage points, which corresponds to a 13.3% relative increase. At the mid-load of 2.22 kW, diesel records 22.5% while BPO50 attains 24.2% (an absolute gain of 1.7, or 7.6% relatively). At full load (3.70 kW), diesel gives 24.8% and BPO50 reaches 26.4%, an absolute increase of 1.6 (≈6.5% relative). Looking across blends at

full load, the BTEs are: diesel 24.8%, BPO10 24.9%, BPO20 25.4%, BPO30 25.8%, BPO40 26.1%, and BPO50 26.4% showing a monotonic rise in efficiency with higher BPO content.

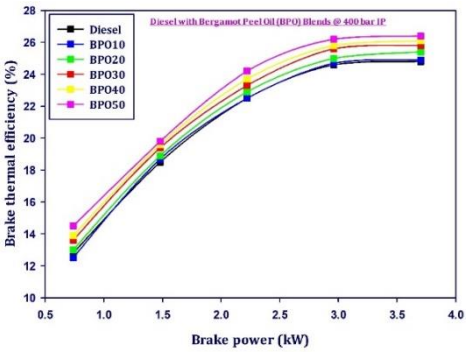

Fig. 8. BTE of BPO-Diesel blends Fig.

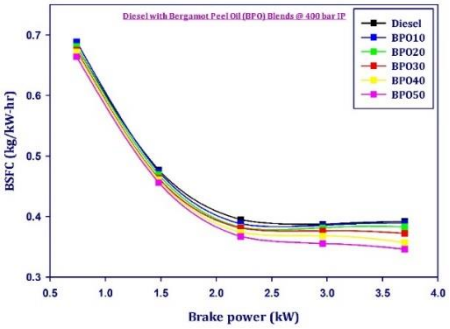

Fig. 9. BSFC of BPO-Diesel blends.

The observed enhancement in thermal efficiency with BPO addition can be explained by a combination of physicochemical and combustion effects. First, BPO contains a substantial fraction of oxygenated organic compounds (from GC–MS/FTIR), which supplies local oxygen within spray/film regions and reduces the extent of fuel-rich pockets, thereby promoting more complete oxidation and increasing the useful heat release. Second, the measured calorific value of BPO (44.05 MJ/kg) is higher than diesel (42.30 MJ/kg), so, per unit mass, BPO contributes slightly more chemical energy—this raises the energy available for conversion to brake work. Third, BPO's lower kinematic viscosity (1.62 mm^2/s vs 2.57 mm^2/s for diesel) improves atomization in the injector nozzle, giving finer droplets and faster evaporation; improved vaporization enhances premixed combustion fraction and reduces losses from incomplete combustion. These three factors act together to increase BTE as the BPO fraction rises.

A cautionary point is the low cetane index of BPO (25 vs 49 for diesel), which tends to increase ignition delay. The data suggest that under the test conditions, this disadvantage is more than offset by the oxygenation, calorific, and atomization benefits—hence even higher blends show superior BTE. At the lowest load, the smallest blend (BPO10) is marginally below diesel (12.5% vs 12.8%), likely because the lower charge temperature and weaker mixing at light load amplify ignition-delay penalties for small oxygenated-blend fractions; however, with increased load and temperature, the benefits dominate, and every blend outperforms diesel for higher BPO fractions. In summary, the BTE results indicate that incorporating BPO into diesel improves thermal efficiency in a load-dependent manner, with larger BPO fractions (notably BPO40–BPO50) delivering the greatest gains (≈6–13% relative improvement depending on load).

The BSFC variation with load for neat diesel and the BPO–diesel blends is summarized in Fig. 9. All fuels generally show lower BSFC as load increases (improved conversion of fuel energy to brake work and smaller relative heat/pumping losses). Neat diesel BSFC decreases from 0.681 kg/kW·h at the lowest load (0.74 kW) to 0.387 kg/kW·h at 2.96 kW, with a slight rise to 0.392 kg/kW·h at the highest load (3.70 kW). In contrast,

BPO blends—especially those with higher BPO fractions—exhibit lower BSFC than diesel across most loads and maintain a more consistent reduction toward high loads; the BPO50 blend records the lowest BSFC values across the range (0.664 → 0.346 kg/kW·h from low to full load). The benefit of increasing the BPO fraction is clear and load-dependent. At full load (3.70 kW), BSFC falls from 0.392 kg/kW·h (diesel) to 0.346 kg/kW·h (BPO50), an absolute reduction of 0.046 kg/kW·h, which is an ~11.7% improvement. At 2.96 kW, the BPO50 blend gives 0.355 kg/kW·h versus diesel 0.387 kg/kW·h (an 8.3% improvement), and at 2.22 kW it drops from 0.395 to 0.367 kg/kW·h (≈7.1% improvement). Even at the lowest load, the largest blend (BPO50) consumes less fuel than diesel (0.664 vs. 0.681 kg/kW·h, a 2.5% reduction). Intermediate blends show intermediate gains (e.g., BPO40 reduces BSFC by ~4.9–8.9% depending on load), while BPO10 is nearly parity with diesel or slightly worse at the lowest load (0.689 vs. 0.681 kg/kW·h, a 1.2% increase).

The observed reductions in BSFC with higher BPO content can be explained by a combination of physicochemical and combustion phenomena. First, BPOs measured higher calorific value (44.05 MJ/kg vs. diesel's 42.30 MJ/kg) supplies more chemical energy per unit mass, which lowers the mass of fuel required to produce the same brake power. Second, the oxygenated composition of BPO improves local oxidation in fuel-rich zones and reduces incomplete combustion losses (CO/HC), effectively increasing the fraction of fuel energy converted to useful work. Third, lower kinematic viscosity of BPO improves spray breakup and atomization through the injector, producing finer droplets that evaporate and mix faster — particularly beneficial at elevated in-cylinder temperatures — thus raising combustion efficiency and reducing BSFC. These three effects act together and become more pronounced with increasing BPO fraction, explaining why blends with higher BPO percentages consistently achieve lower BSFC. A few practical observations merit note: the slight BSFC increase of neat diesel between 2.96 and 3.70 kW (0.387 → 0.392 kg/kW·h) may reflect experimental scatter or a shift away from the engine's most favorable operating point under our test conditions; blends, particularly BPO40–BPO50, do not show this uptick and continue to improve. The small BSFC penalty for BPO10 at the lowest load likely stems from the interplay between the low cetane index of BPO (longer ignition delay) and low charge temperatures at light load, which can temporarily worsen combustion efficiency; as load (and charge temperature) increases, the atomization/oxygenation benefits dominate and BSFC improves. In summary, the BSFC data corroborate the BTE results: higher BPO substitution reduces specific fuel consumption significantly (up to ~12% at full load for BPO50), indicating improved fuel utilization.

IV.ii.b. In-cylinder pressure and Heat release rate characteristics

The variation of in-cylinder pressure with respect to crank angle (CA), shown in fig. 10, for diesel and BPO blends indicates a significant influence of fuel properties on combustion behavior. With an increasing proportion of BPO in the blend, the rate of pressure rise is observed to increase, leading to slightly higher peak pressures compared to pure diesel operation. The peak in-cylinder pressures recorded for diesel, BPO10, BPO20, BPO30, BPO40, and BPO50 are 65.9 bar, 67.3 bar, 69.02 bar, 69.1 bar, 70.0 bar, and 70.1 bar, respectively. This enhancement in peak pressure can be attributed to the improved oxygen content in BPO, which promotes better combustion, and the higher

calorific value of the blends, which releases more energy during the combustion process. Additionally, the slightly higher latent heat of vaporization of BPO influences mixture formation and temperature conditions inside the cylinder.

However, the start of combustion (SOC) for BPO blends is retarded compared to diesel, primarily due to the lower cetane rating of BPO, which increases the ignition delay. Consequently, the crank angle position corresponding to peak pressure also shifts towards a later phase as the BPO content increases. While diesel and BPO10 exhibit peak pressure at the same crank angle position, BPO20 shows a retardation of 1° CA, BPO30 and BPO40 exhibit a 2° CA delay, and BPO50 records the maximum delay of 3° CA relative to diesel. The delayed SOC results in more fuel accumulating in the premixed combustion phase, contributing to the observed higher pressure rise and peak cylinder pressure for BPO blends despite the retarded combustion phasing.

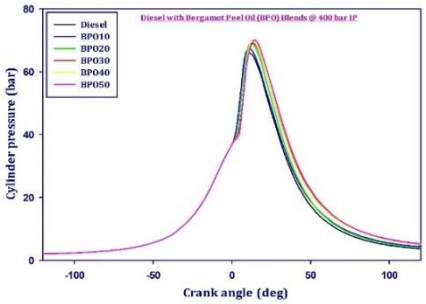

Fig. 10 In-cylinder pressure of BPO-Diesel blends

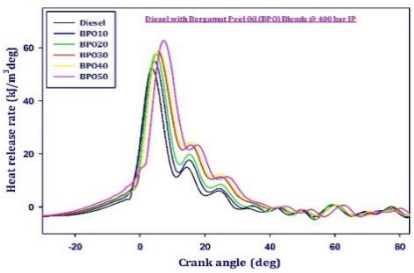

Fig. 11 Heat release rate of BPO-Diesel blends

Fig. 11 shows the trend of HRR of Diesel-BPO blends. The peak HRR for diesel, BPO10, BPO20, BPO30, BPO40, and BPO50 was measured as 52.1, 54.7, 57.8, 58.2, 58.9, and 62.6 $kJ \cdot m^{-3} \cdot deg^{-1}$, respectively. Compared to diesel, the peak HRR increases progressively with higher BPO fraction by approximately +5.0%, +10.9%, +11.7%, +13.1% and +20.2% for BPO10 to BPO50, respectively. The crank-angle at which the peak HRR occurs is retarded for all BPO blends relative to diesel, i.e., the peak HRR is reached later in the expansion stroke, in the same way the peak in cylinder pressure was observed to be retarded.

The authors attribute the systematic retardation of the peak HRR primarily to the lower cetane index (or lower ignition quality) of the BPO blends compared with neat diesel. Lower cetane results in longer ignition delay (time between start of injection and onset of auto-ignition). A longer ignition delay causes more fuel to accumulate in the cylinder before the onset of high-temperature combustion; when ignition finally occurs, a larger premixed charge burns rapidly. That larger premixed fraction produces a steeper HRR rise and a larger instantaneous peak HRR — but because ignition is delayed, the entire HRR trace (including its maximum) shifts to a later crank angle (retarded timing). This explains both the higher peak magnitude and the later occurrence of the peak HRR observed with increasing BPO fraction. In addition to ignition delay effects, the authors note fuel chemistry effects. The BPO blends here exhibit a higher effective calorific contribution per unit of fuel delivered (as highlighted earlier for peak pressure), and many bio-oils contain oxygenated species, which can alter flame speed and local burning intensity. Higher gross energy available to the burning zone increases the

instantaneous heat release when combustion proceeds, contributing to the observed higher peak HRR values for BPO blends. Combined with the larger premixed burn fraction caused by ignition delay, this elevates the peak HRR further.

BPO's volatility and physical properties (viscosity and surface tension differences from diesel) change atomization and spray breakup. If BPO blends produce coarser droplets or slower vaporization under the tested conditions, more liquid fuel can survive until ignition and then evaporate rapidly during the ignition delay. This increases the premixed-like energy available at ignition and produces a more abrupt HRR rise (steeper HRR slope) and a higher peak. Conversely, if BPO improves micro-mixing and flame propagation locally (via oxygen content), it can also strengthen the peak HRR; both mechanisms are consistent with the measured trend. Heat release drives cylinder pressure rise. A retarded HRR peak, therefore, naturally leads to a retarded peak pressure, and vice versa, the two are tightly coupled through in-cylinder thermodynamics. Because more energy is released in a shorter crank-angle window (larger premixed burn), the pressure rise is correspondingly sharper, but it happens later, which matches the observation that peak HRR and peak pressure are retarded together for BPO blends.

The percent increases show near-monotonic growth of peak HRR with blend fraction, with BPO50 showing the largest change (~+20%). This nonlinearity at higher blend ratios suggests that ignition-quality and fuel-property effects compound — beyond a certain BPO fraction, the ignition delay and premixed fraction increase enough that the peak HRR climbs more rapidly. This should flag a regime where further increases in blend fraction could significantly shift combustion phasing and require retarded injection/timing correction to preserve desired work output and emissions.

The larger peak HRR and steeper initial slope indicate an increased premixed combustion fraction and faster burn rates. The area under the HRR curve (total heat released) will reflect total fuel energy; a higher peak with similar integrated area primarily indicates faster concentrated release rather than more total energy. Therefore, the peak magnitude and rise rate are as important as the timing of the peak for diagnosing combustion mode changes induced by BPO blending.

IV.ii.c. CO and HC emission

Fig. 12 shows the CO emission of BPO-Diesel blends. It is observed that carbon monoxide (CO) emissions consistently decreased with the increase in BPO blend ratio when compared to diesel fuel. For neat diesel, CO emissions varied between 0.09 and 0.54 g/kWh across the measured operating conditions, whereas for the highest blend (BPO50), the corresponding values ranged from 0.07 to 0.40 g/kWh. At the highest load condition, CO reduced from 0.54 g/kWh for diesel to 0.40 g/kWh for BPO50, representing a reduction of approximately 25.9%. Similar decreasing trends were recorded at intermediate loads. However, at the lowest operating condition, BPO10 showed a marginal increase in CO relative to diesel, which can be attributed to differences in atomization and evaporation characteristics at low combustion temperatures. Beyond BPO10, the CO reduction trend became more consistent, indicating the dominant influence of BPO's inherent oxygenation on combustion chemistry.

The primary reason for this downward trend in CO emissions is the oxygenated nature of BPO. Unlike diesel, BPO contains a significant proportion of chemically bound oxygen within its molecular structure. This additional oxygen improves local stoichiometry in rich combustion zones, thereby accelerating the oxidation of CO to CO_2 during the later stages of combustion. In conventional diesel combustion, oxygen deficiency in localized rich pockets often leads to incomplete oxidation and higher CO emissions. By supplying internal oxygen, BPO minimizes the occurrence of such oxygen-lean regions, resulting in more complete combustion. This mechanism becomes particularly effective under high-load conditions where diffusion-controlled burning dominates, and oxygen deficiency would normally be severe.

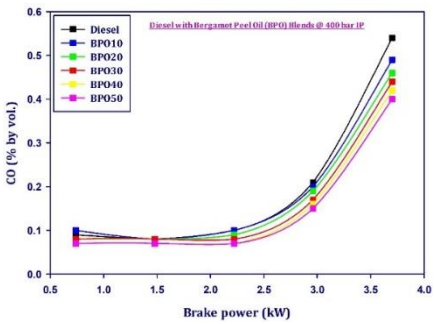

Fig. 12. CO emission of BPO-Diesel blends

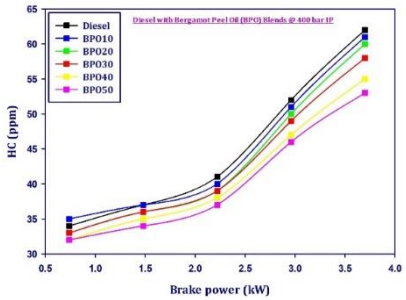

Fig. 13. HC emission of BPO-Diesel Blends

Another contributing factor is the enhanced radical pool, particularly hydroxyl (OH) radicals, generated during the combustion of oxygenated fuels. The presence of BPO facilitates reactions such as $CO + OH \rightarrow CO_2 + H$, which effectively oxidize CO into CO_2. This radical-assisted pathway is strongly temperature-dependent, and the HRR analysis revealed that BPO blends exhibit higher peak heat release rates compared to diesel. This indicates that a larger fraction of fuel burns rapidly during the premixed phase, creating localized high-temperature zones conducive to CO oxidation. Thus, the chemical reactivity and radical formation associated with oxygenated molecules in BPO substantially improve oxidation kinetics.

Although BPO blends exhibit longer ignition delays due to their lower cetane index, which results in retarded combustion phasing, this does not lead to higher CO emissions as might be expected. Typically, delayed combustion can reduce the available time for complete oxidation of CO before exhaust valve opening. However, in this case, the extended ignition delay also increases the amount of premixed fuel available for rapid combustion once ignition starts. This premixed combustion phase is highly exothermic and elevates local temperatures significantly. Higher local temperatures accelerate oxidation reactions and reduce CO concentration, offsetting the disadvantage of shorter residence time at peak pressure. Therefore, the longer ignition delay combined with BPO's inherent oxygenation produces a net decrease in CO emissions.

The degree of CO reduction becomes more pronounced with increasing engine load. At higher loads, the baseline CO emissions for diesel rise sharply due to richer equivalence ratios and insufficient oxygen availability in diffusion flames. Under these conditions, the oxygenated nature of BPO provides a distinct advantage by improving oxidation

even in fuel-rich pockets, leading to reductions as high as 25–26% for BPO50. At the lowest operating point, however, BPO10 recorded a slightly higher CO emission than diesel. This anomaly can be attributed to changes in physical properties such as higher viscosity and surface tension of BPO blends, which may have adversely affected spray atomization and vaporization at low combustion temperatures. Consequently, local quenching and incomplete oxidation could have contributed to the marginal CO rise at light load. Nevertheless, as the blend ratio and cylinder temperature increase, the beneficial chemical effects of BPO overshadow the physical property drawbacks.

Fig. 13 shows the trends of HC emission for Diesel-BPO blends. It is observed a clear, monotonic reduction in hydrocarbon (HC) emissions was observed as the BPO fraction increased, especially at mid-to-high operating points. Across the five test points, the average HC change vs. diesel is negligible for BPO10 (~ +0.6% mean change), but progressively larger reductions appear for higher blends: BPO20 ≈ −3.5%, BPO30 ≈ −4.6%, BPO40 ≈ −7.9%, and BPO50 ≈ −10.0%. The load dependence is also notable: at the highest operating point, HC falls from 62 (diesel) to 53 (BPO50) — an absolute drop of 9 units, which is ≈14.5%. The reductions are small at light load but become pronounced at higher loads and with higher BPO fractions.

The dominant mechanistic explanation is fuel-bound oxygen. BPO molecules carry chemically bound oxygen that becomes available in locally rich regions where gas-phase oxygen is limited. This internally supplied oxygen helps oxidize partially burned hydrocarbons (RH radicals and CO intermediates) to CO_2 during the combustion event. In diffusion-controlled pockets—common at higher loads—this extra oxygen reduces the population of unburned hydrocarbons that would otherwise escape as HC. This explains why HC reduction becomes larger with increasing BPO fraction and is most effective at higher loads. Oxygenated fuels tend to promote the formation of active radicals (notably OH), which directly participate in HC oxidation pathways (e.g., abstraction and oxidation sequences converting large hydrocarbon fragments ultimately to CO and CO_2). The HRR/pressure results showed stronger, steeper premixed burns with higher BPO content (higher peak HRR). Those concentrated combustion events generate locally higher instantaneous temperatures and a richer OH-radical pool during the premixed phase, accelerating the conversion of intermediate hydrocarbon fragments to stable products and thereby lowering HC emissions.

The BPO blends show longer ignition delay (lower cetane index) and a retarded combustion phasing. Longer ignition delay increases the premixed fraction; a larger premixed burn can enhance oxidation completeness if mixing and evaporation are adequate — this promotes HC reduction. Conversely, if mixing is poor or wall-wetting occurs, ignition delay can increase quenching and HC formation. In the present dataset, the net effect is HC reduction for blends ≥BPO20, indicating that the chemical benefits (fuel oxygen + enhanced radical chemistry + higher premixed temperatures) overcome the potential disadvantages of later phasing in this engine-test regime. At the lowest test point, BPO10 shows a tiny increase in HC (35 vs 34 for diesel). This small anomaly can be explained by physical-property effects at low temperatures: modest additions of BPO can alter viscosity, surface tension, and volatility, degrading spray atomization or slowing vaporisation under low-load, low-temperature conditions. That leads to local liquid-film formation or wall-wetting and slightly higher HC. As the BPO fraction and

cylinder temperatures increase, fuel oxygenation and improved gas-phase chemistry dominate, and the HC drops. Measurement scatter at very low absolute HC levels may also contribute to the tiny variation seen for BPO10. The largest absolute and percentage HC reductions occur at higher loads and for higher BPO fractions (e.g., BPO50 gives ~14.5% reduction at the highest load). At higher loads, the combustion mode shifts toward diffusion-controlled burning with more local rich pockets — the precise scenario where fuel-bound oxygen and improved radical chemistry provide the greatest marginal benefit. In addition, the compounding of effects (increasing premixed fraction, greater instantaneous HRR, and more oxygen from fuel) produces a non-linear improvement with blend ratio, which explains why BPO40 and BPO50 show disproportionately larger HC decreases.

IV.ii.d. NO emission

Fig. 14 shows the trends of NO emission of Diesel-BPO blends. It is observed that a clear and systematic increase in NO emissions with increasing BPO fraction across all tested operating points. The increase is monotonic with blend ratio: BPO10 shows a small average rise (≈+5.7%), while BPO20, BPO30, BPO40, and BPO50 show progressively larger average increases of ≈+10.0%, +14.0%, +22.3% and +28.0%, respectively (averages computed across the five operating points). In absolute terms, the mean NO rise relative to diesel is ≈ +15.2, +30.0, +41.8, +70.6, and +94.6 units for BPO10→BPO50. The NO increases from 147 to 250 ppm (diesel → BPO50) at the lightest operating point (≈+70.1%) and from 682 → 799 at the heaviest operating point (≈+17.2%). Thus, while percentage increases are largest at light load (because the diesel baseline is small there), significant NO increases are observed across the entire load range and become substantial for higher BPO fractions.

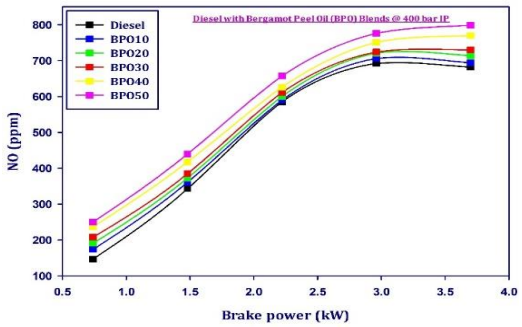

Fig. 14. NO emission of BPO-Diesel blends

The principal mechanism driving the NO rise is thermal NO formation (the extended Zeldovich mechanism), which is extremely sensitive to local flame temperature; reaction rates increase exponentially with temperature. From the HRR and pressure analysis, we know that BPO blends produce higher peak HRR and larger instantaneous heat release during the premixed burn. These concentrated heat-release events generate higher local instantaneous temperatures in the burning zones. Even though the HRR/pressure peaks are retarded in crank angle, their peak magnitudes are higher; the net effect is higher maximum temperatures at some point during the cycle, which strongly promotes thermal NO formation and explains the NO increases measured.

BPO is oxygenated. The fuel-bound oxygen and the altered chemical structure promote a richer radical pool (O, H, OH) during combustion. Elevated concentrations of O and OH accelerate pathways that convert N_2 into NO (e.g., $O + N_2 \rightarrow NO + N$ and subsequent chain reactions), and generally speed up the high-temperature chemistry leading to thermal NO. In addition, oxygenated fuels tend to support more complete and faster oxidation locally, while beneficial for CO and HC also raises the instantaneous temperature and radical concentrations, again favoring NO formation. Retarded combustion phasing (observed for BPO blends) sometimes reduces NO because the highest heat release occurs later in the expansion stroke, where gas densities and temperatures are lower. However, in this dataset, the magnitude of heat release during the premixed burn increases enough that the instantaneous peak temperatures are higher despite the retardation. Consequently, the temperature-driven NO formation mechanism dominates the phasing effect and causes a net increase in NO for all blends, especially at higher blend ratios.

The BPO-induced changes in physical properties (viscosity, volatility, and spray characteristics) alter droplet breakup and vaporization. Better evaporation and more homogeneous premixing can reduce local rich pockets (reducing soot) but can create larger stoichiometric / near-stoichiometric zones during the premixed burn, where temperatures are maximized, again favoring NO. Conversely, any deterioration in atomization that produces persistent rich pockets would normally increase soot rather than NO. The observed simultaneous decrease in CO/HC and increase in NO is consistent with improved oxidation/temperature effects rather than with worse mixing. Percentage increases are largest at light load (e.g., ~+70% at the lightest point for BPO50) because baseline NO with diesel is small there; however, absolute NO increases are larger at mid/high loads. For example, BPO50 increases NO by +103 units at the lightest point and +117 units at the highest point, both large in absolute terms. This pattern indicates the BPO chemistry enhances NO production across the map, but percent metrics must be interpreted with the baseline in mind. Fuel-bound nitrogen (fuel-NOx) is unlikely to be a major contributor here because typical vegetable/fruit bio-oils have low nitrogen content; therefore, the observed increase is not expected to be driven by fuel-N chemistry but rather by thermal and possibly prompt NO (prompt NO being associated with hydrocarbon radical–N_2 interactions near stoichiometric flames). Given the stronger premixed stoichiometric burns and larger radical pools with BPO, prompt NO could give a modest additional contribution, but thermal NO remains the dominant source.

IV.ii.v. Smoke emission

Fig. 15 shows the smoke emission trends of BPO-Diesel blends. The smoke emission for pure diesel is consistently higher compared to all BPO blends across the entire load range. As the proportion of BPO in the blend increases from 10% (BPO10) to 50% (BPO50), the smoke opacity decreases significantly. At 0.74 kW load, smoke reduces from 14.3 HSU (Diesel) to 11.6 HSU (BPO50). At 3.7 kW load, smoke reduces from 43.7 HSU (Diesel) to 37.3 HSU (BPO50). This represents an approximate 14% reduction at full load when 50% BPO is used. The primary factors influencing the smoke emission trend are: BPO contains inherent oxygen molecules in its chemical structure, which promote better oxidation of the fuel-air mixture during combustion. Smoke

primarily consists of unburnt carbon particles formed in locally fuel-rich regions. The presence of oxygen in BPO assists in oxidizing these carbon particles into CO_2, thereby reducing the formation of soot. Diesel typically contains a certain proportion of aromatics and sulfur compounds, which favor soot nucleation and growth during combustion. In contrast, BPO, being a bio-based oxygenated fuel, has lower aromatic content and negligible sulfur, reducing the tendency of soot precursor formation. BPO has a lower viscosity compared to diesel, which leads to better atomization of fuel droplets upon injection. Finer droplets increase the surface area-to-volume ratio, ensuring more efficient fuel-air mixing. Enhanced atomization reduces the probability of localized rich zones where soot formation typically occurs. BPO has a lower C/H ratio than conventional diesel. Since smoke is essentially carbonaceous matter, a lower carbon content naturally results in reduced soot formation. Additionally, higher hydrogen content enhances flame temperature, promoting complete oxidation of carbon.

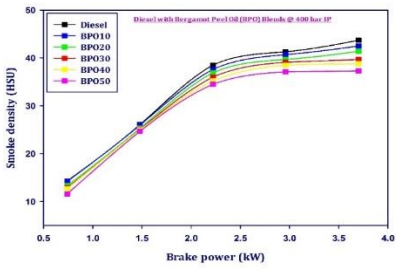

Fig. 15. Smoke emission of BPO-Diesel Blends

Smoke emissions increase with increasing engine load for all fuels, but the rate of increase is less for BPO blends compared to diesel. This is because, at higher loads, fuel injection quantity increases, leading to richer mixtures and a tendency for incomplete combustion. However, the oxygenated nature of BPO mitigates this effect by supporting better oxidation; hence, the smoke reduction effect is more pronounced at full load (3.7 kW) compared to part load (0.74 kW). At 0.74 kW, diesel = 14.3 HSU, BPO50 = 11.6 HSU (difference = 2.7 HSU). At 3.7 kW, diesel = 43.7 HSU, BPO50 = 37.3 HSU (difference = 6.4 HSU). This demonstrates that the benefit of BPO blending becomes more significant at higher loads, where the tendency for smoke is higher.

The BPO10 and BPO20 show a moderate reduction in smoke compared to diesel. BPO30 and BPO40 exhibit a noticeable drop as oxygen availability improves further. BPO50 gives the lowest smoke emissions, confirming that a higher proportion of oxygenated fuel effectively reduces soot formation. The reduction in smoke emissions with BPO blending is primarily due to oxygen enrichment, improved atomization, better combustion quality, and lower carbon content of the fuel. These factors collectively minimize the formation of soot precursors and enhance the oxidation of any incipient soot particles.

V. Conclusion

In the present experimental study, the feasibility of utilizing BPO as an alternative fuel to diesel was investigated in a compression ignition engine under various blending ratios (BPO10, BPO20, BPO30, BPO40, and BPO50) without any major engine modifications. The analysis covered performance, combustion, and emission

characteristics, with specific attention to in-cylinder pressure variation, heat release rate, and exhaust emissions compared to baseline diesel operation. The primary objective was to assess the impact of BPO's oxygenated nature, high volatility, and energy content on engine behavior and to determine its potential as a sustainable substitute for diesel fuel. The key findings of the study are as follows:

I. BTE improved with BPO addition due to the oxygenated nature of the fuel, which enhanced combustion. Maximum improvement of 3–6% was observed for BPO30–BPO40 blends compared to diesel.
II. BSFC **decreased** for all BPO blends owing to their **higher calorific value**, which provided more energy per unit of fuel consumed. A reduction of **5–9%** was observed for higher blends like **BPO40 and BPO50**.
III. Higher BPO proportions resulted in increased peak cylinder pressure and RoPR. BPO50 recorded the highest peak pressure, attributed to better oxidation and higher local temperatures.
IV. Ignition delay increased marginally for higher blends due to the lower cetane number. Overall combustion duration remained close to diesel because oxygen content accelerated flame propagation.
V. Significant reduction in smoke opacity was recorded, up to 14–17% for BPO50. This is due to enhanced soot oxidation promoted by fuel-bound oxygen.
VI. Both CO and HC decreased by 8–12% with BPO blends compared to diesel. Improved atomization and better mixing contributed to complete combustion.
VII. NOx emissions increased by 6–10% for higher BPO blends. This rise is attributed to higher in-cylinder temperature and oxygen availability, enhancing thermal NO formation.

Overall, it can be concluded that although BPO50 exhibited the greatest improvements in performance and emissions, its low viscosity and low cetane number raise concerns related to fuel lubricity and combustion stability. These factors contribute to increased ignition delay, which can lead to undesirable effects such as knocking or abnormal combustion at higher loads. Considering these limitations, BPO40 is recommended as the most suitable blend for CI engine applications, as it offers an optimal balance between improved thermal efficiency, reduced emissions, and safe engine operation without requiring significant modifications.

VI. Future Scope

Further research can be directed towards addressing the limitations observed with higher BPO blends. The inclusion of cetane improvers can significantly reduce ignition delay and mitigate the adverse effects of combustion phasing associated with low cetane numbers. Additionally, integrating after-treatment systems such as Selective Catalytic Reduction (SCR) or Exhaust Gas Recirculation (EGR) can effectively control NO_x emissions while maintaining improved performance characteristics. Furthermore, optimization of fuel injection strategies, including injection timing and pressure adjustments, can enhance combustion efficiency and prevent knocking, enabling wider adoption of BPO blends without compromising engine durability and reliability.

Conflict of Interest:

There was no relevant conflict of interest regarding this article.

References

I. Ashok, B., R. Thundil Karuppa Raj, et al. "Lemon Peel Oil – A Novel Renewable Alternative Energy Source for Diesel Engine." *Energy Conversion and Management* 139 (2017): 110–121. 10.1016/j.enconman.2017.02.049

II. Chen, Hui et al. "The Effect of a Pine Oil/Diesel Blend on the Particulate Emission Characteristics of a Diesel Engine under a Pre-Injection Strategy with EGR." *Sustainable Energy & Fuels* 7.15 (2023): 3644–3653. Web. 17 Aug. 2025. https://pubs.rsc.org/en/content/articlehtml/2023/se/d3se00581j

III. Chivu, Robert Mădălin et al. "Assessment of Engine Performance and Emissions with Eucalyptus Oil and Diesel Blends." *Energies 2024, Vol. 17, Page 3528* 17.14 (2024): 3528. Web. 17 Aug. 2025. https://www.mdpi.com/1996-1073/17/14/3528/htm

IV. Doppalapudi, Arun Teja, Abul Kalam Azad, and Mohammad Masud Kamal Khan. "Exergy, Energy, Performance, and Combustion Analysis for Biodiesel NOx Reduction Using New Blends with Alcohol, Nanoparticle, and Essential Oil." *Journal of Cleaner Production* 467 (2024): 142968. Web. 17 Aug. 2025. https://www.sciencedirect.com/science/article/pii/S095965262402417X

V. Duraisamy, Ganesh, Murugan Rangasamy, and Abul K. Hossain. "A Study on Flexible Dual-Fuel and Flexi Combustion Mode Engine to Mitigate NO, Soot and Unburned Emissions." *Fuel* 322 (2022): 124276. Web. 19 Aug. 2025. https://www.sciencedirect.com/science/article/abs/pii/S0016236122011280

VI. Ellappan, Sivakumar, and Silambarasan Rajendran. "A Comparative Review of Performance and Emission Characteristics of Diesel Engine Using Eucalyptus-Biodiesel Blend." *Fuel* 284 (2021): 118925. Web. 17 Aug. 2025. https://www.sciencedirect.com/science/article/abs/pii/S0016236120319219

VII. Gad, M. S. et al. "Combustion Characteristics of a Diesel Engine Running with Mandarin Essential Oil -Diesel Mixtures and Propanol Additive under Different Exhaust Gas Recirculation: Experimental Investigation and Numerical Simulation." *Case Studies in Thermal Engineering* 26 (2021): 101100. Web. 17 Aug. 2025. https://www.sciencedirect.com/science/article/pii/S2214157X2100263X

VIII. Karthickeyan, V. et al. "Simultaneous Reduction of NOx and Smoke Emissions with Low Viscous Biofuel in Low Heat Rejection Engine Using Selective Catalytic Reduction Technique." *Fuel* 255 (2019): 115854. Print.

IX. Nanthagopal, K. et al. "Lemon Essential Oil - A Partial Substitute for Petroleum Diesel Fuel in Compression Ignition Engine." *International Journal of Renewable Energy Research* 7.2 (2017): 467–475. Print.

X. Nguyen, Van Nhanh et al. "Engine Behavior Analysis on a Conventional Diesel Engine Combustion Mode Powered by Low Viscous Cedarwood Oil/Waste Cooking Oil Biodiesel/Diesel Fuel Mixture – An Experimental Study." *Process Safety and Environmental Protection* 184 (2024): 560–578. Web. 17 Aug. 2025. https://www.sciencedirect.com/science/article/abs/pii/S0957582024001253

XI. Patel, Ashok K., Basant Agrawal, and B. R. Rawal. "Assessment of Diesel Engine Performance and Emission Using Biodiesel Obtained from Eucalyptus Leaves." *European Journal of Sustainable Development Research* 7.1 (2023): em0210. Web. 17 Aug. 2025. https://www.ejosdr.com.https://doi.org/10.29333/ejosdr/12749

XII. Vallinayagam, R., S. Vedharaj, W. M. Yang, P. S. Lee, et al. "Combustion Performance and Emission Characteristics Study of Pine Oil in a Diesel Engine." *Energy* 57 (2013): 344–351. Web. 10.1016/j.energy.2013.05.061

XIII. Vallinayagam, R., S. Vedharaj, W. M. Yang, P. S. Lee, et al. "Operation of Neat Pine Oil Biofuel in a Diesel Engine by Providing Ignition Assistance." *Energy Conversion and Management* 88 (2014): 1032–1040. Web. 10.1016/j.enconman.2014.09.052

XIV. Y. Alex, et al. "Study of Engine Performance and Emission Characteristics of Diesel Engine Using Cerium Oxide Nanoparticles Blended Orange Peel Oil Methyl Ester." *Energy Nexus* 8 (2022): 100150. Web. 17 Aug. 2025. https://www.sciencedirect.com/science/article/pii/S277242712200105X